frontiers | Frontiers in Earth Science

ORIGINAL RESEARCH
published: 11 May 2022
doi: 10.3389/feart.2022.882701

Experimental Insights Into the *In Situ* Formation and Dissociation of Gas Hydrate in Sediments of Shenhu, South China Sea

Qian Zhang[1,2,3], *Xuwen Qin*[4,5], *Hong Zhang*[1,2,3], *Yanhui Dong*[1,2,3]*, *Cheng Lu*[4,5,6], *Shouding Li*[1,2,3], *Luokun Xiao*[1,2,3], *Chao Ma*[4,5] *and Hang Bian*[6,7]

[1]*Key Laboratory of Shale Gas and Geoengineering, Institute of Geology and Geophysics, Chinese Academy of Sciences, Beijing, China,* [2]*University of Chinese Academy of Sciences, Beijing, China,* [3]*Innovation Academy for Earth Science, Chinese Academy of Sciences, Beijing, China,* [4]*Guangzhou Marine Geological Survey, China Geological Survey, Guangzhou, China,* [5]*National Engineering Research Center of Gas Hydrate Exploration and Development, Guangzhou, China,* [6]*Center of Oil & Natural Gas Resource Exploration, China Geological Survey, Beijing, China,* [7]*School of Energy Resources, China University of Geosciences, Beijing, China*

Natural gas hydrates as sustainable energy resources are inherently affected by mineral surfaces and confined spaces in reservoirs. However, the habits of hydrates in geological sediments are still an open question. In this work, we systemically studied the process of hydrate formation and dissociation in sediments from the Shenhu area of the South China Sea to examine the evolution of hydrate saturation and permeability in sediments and their relationship. Characterization of samples indicates that sediments of the Shenhu area are mainly composed of clay and fine sand grains and provide a large number of nanopores for hydrate accumulation. For *in situ* observations enabled by low-field nuclear magnetic resonance methods, the formation of hydrates shows a different kinetic behavior with an induction time compared to hydrate dissociation. Estimated by variations of hydrate saturation (%) over time, the rate of hydrate formation is around 12%/min, while the dissociation rate increases to 3%/min with the higher temperature. With the presence of hydrates, pore space and thus permeability of sediments decreased obviously by one and three orders of magnitude when the hydrate saturation is 20 and 45%, respectively. Compared to models with the assumption of grain-coating and pore-filling hydrates, the tendency of permeability evolution from NMR measurements is between fitted lines from models. It highlights that the existing models considering a single pattern of hydrate growth cannot precisely describe the relationship between permeability and hydrate saturation. Hybrid hydrate habits coexist in sediments resulting from heterogeneous pore structures and thus complex gas–water distributions.

Keywords: gas hydrate, sediment, formation and dissociation, nuclear magnetic resonance, pore habit

OPEN ACCESS

Edited by:
Zhifeng Wan,
Sun Yat-sen University, China

Reviewed by:
Chao Fu,
China National Offshore Oil Corporation (China), China
Yanbin Yao,
China University of Geosciences, China

***Correspondence:**
Yanhui Dong
dongyh@mail.iggcas.ac.cn

Specialty section:
This article was submitted to Marine Geoscience, a section of the journal Frontiers in Earth Science

Received: *24 February 2022*
Accepted: *04 April 2022*
Published: *11 May 2022*

Citation:
Zhang Q, Qin X, Zhang H, Dong Y, Lu C, Li S, Xiao L, Ma C and Bian H (2022) Experimental Insights Into the In Situ Formation and Dissociation of Gas Hydrate in Sediments of Shenhu, South China Sea. Front. Earth Sci. 10:882701. doi: 10.3389/feart.2022.882701

INTRODUCTION

Gas hydrates are ice-like compounds composed of hydrogen-bound water molecules and low molecular weight gases that are stable at high pressure and low temperature. Natural gas hydrates (NGHs) are primarily distributed in permafrost and sediments and have attracted widespread attention as promising clean and sustainable energy resources (Sloan, 2003; Letcher, 2020). In

particular, the Shenhu area, located in the center of the northern continental slope of the South China Sea (SCS), has become a key target area for marine gas hydrate production with abundant NGH resources (Li et al., 2019).

The Shenhu area in the Pearl River Mouth Basin has sea knolls, submarine canyons, and erosion toughs, and obviously, seabed topography fluctuates with a water depth of 1000~1700 m (Wang et al., 2021). Previous studies indicate that the sea bottom of the Shenhu area has favorable conditions for hydrate formation with a temperature of 2~4°C, a pressure larger than 10 MPa, and the abundant thermogenic gas or biogenic gas for hydrate growth (Su et al., 2016; Liang et al., 2017; Li et al., 2019; Zhang et al., 2019). Moreover, geological bodies including slope fans, slumping blocks, and contour current sedimentation systems are conducive to the accumulation of hydrates. However, a comprehensive understanding of the reservoir characteristics and their impact on hydrate habits in this area is still an open question.

It is increasingly evident that properties of porous media play a critical role in the formation, dissociation, and occurrence of gas hydrates under natural conditions. Compared with homogeneous nucleation processes, hydrate formation can be promoted by the addition of porous media with regard to the lower activation energy, more nucleation sites, and the reduced potential barrier of nucleation (Prasad, 2015; Ghaedi et al., 2016; Andres-Garcia et al., 2019). Previous studies have paid attention to the particle size, distribution, composition of porous media, and their impacts on hydrate habits. In particular, the particle size is a key factor affecting mass transfer performance, hydrate phase equilibrium conditions, and thus the induction time of hydrate formation in geomaterials (Qin et al., 2021). Some scholars believed that the enhancement of heat and mass transfer in porous media with a large particle size facilitates the system to achieve supersaturation and nucleation, which results in a shorter induction time of hydrate (Kumar Saw et al., 2015; Liu et al., 2015). However, others believed that the reduction of induction time can be observed in systems with a smaller particle size because of the larger nucleation area, the greater variation in capillary pressure, and the stronger nucleation (Liu et al., 2015; Siangsai et al., 2015; Heeschen et al., 2016). To date, there is no uniform boundary between small and large particle size, and no consistent conclusion on the effect of the particle size on hydrate nucleation and growth (Qin et al., 2021). In marine sediments, different particle sizes and their ratio result in complex pore structures, which may complicate the processes of hydrate formation and dissociation. Therefore, further experimental investigation in terms of coupled factors regarding pore structural properties on hydrate habits is highly needed.

With the hydrate formation or dissociation, permeability in hydrate-bearing sediments varies subjected to pore structure evolution and has a profound impact on heat and mass transfer and the subsequent dynamics of hydrates (Wang, 2019; Li et al., 2020; Song et al., 2020). Previous studies have demonstrated that the evolution of permeability is highly controlled by sediment features and the saturation and pore habits of hydrate crystals (Ren et al., 2020; Wang et al., 2021; Lu et al., 2021a; 2021b). There are a lot of experimental results

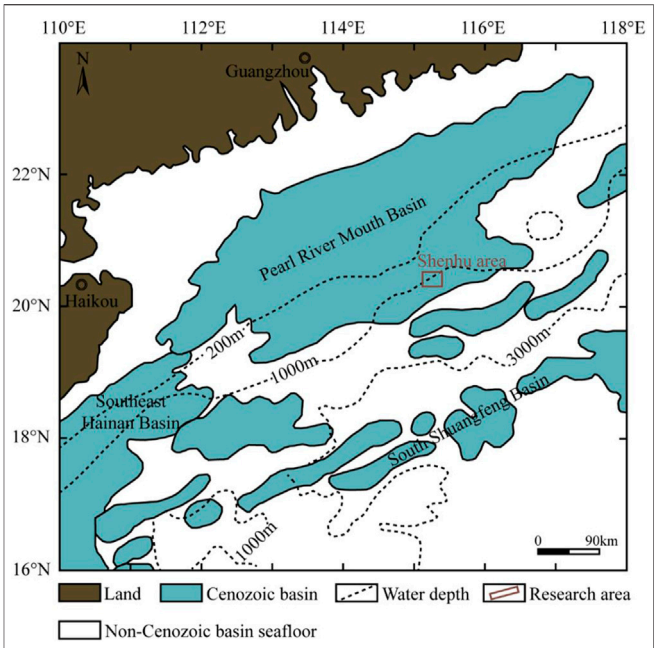

FIGURE 1 | Geological map of the Shenhu area and location of sites drilled. (Modified after Li et al., 2019; Wang et al, 2021).

about hydrate–saturation-dependent permeability in sediments, but the obvious discrepancy is observed as a result of differences in sample types, measurement methods, and experimental conditions (Kuang et al., 2020; Shen et al., 2020; Sun et al., 2021; Wen et al., 2021). Because of the absence of comparable experimental data, theoretical permeability models are developed to estimate the hydrate saturation and permeability relationship in sediments (Kleinberg, 2003; Mahabadi et al., 2016; Kossel et al., 2018). Most of the models are derived using simplified pore space, i.e., straight or tortuous capillary tubes, with the assumption of pore-filling or grain-coating hydrates in pores (Wang et al., 2021; Lei et al., 2022a). Apart from classic models, the hybrid model, modified Corey model, and cubic model are developed to address the hydrate-saturation-dependent permeability (Delli and Grozic, 2014; Lei et al., 2022a). Theoretical models usually include one or multiple uncertain parameters, which can be fitted by a variety of experimental results under different gas–water conditions. Various gas–water supply patterns complicate hydrate pore habits and limit the application of models for permeability prediction (Yin et al., 2018). In particular, gas hydrates mainly cement grain contacts under excess gas conditions, while tend to be as sediment frame components under excess water conditions (Delli and Grozic, 2014). Permeability usually decreases with increasing hydrate saturation; however, the permeability can vary several orders of magnitude regarding different sediment types and conditions even with identical hydrate saturation (Liang et al., 2011; Kang et al., 2016). A mechanistic understanding of permeability in hydrate-bearing sediments with regard to complex pore structure, gas–water conditions, and thus dynamic hydrate pore habits is still lacking.

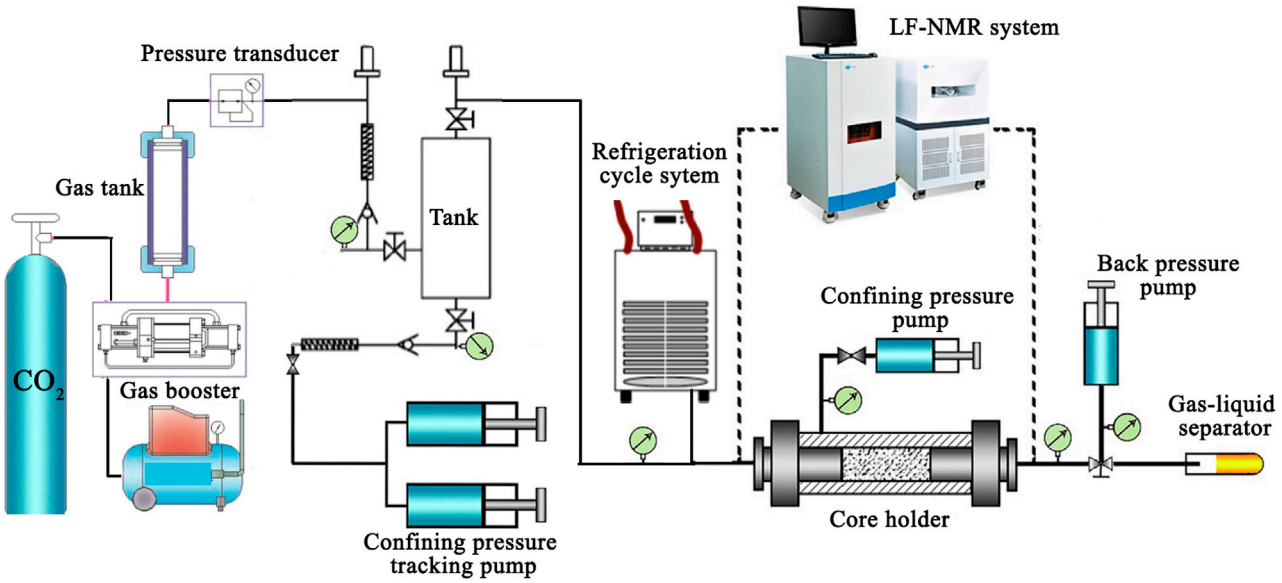

FIGURE 2 | Schematic diagram of the NMR experimental apparatus.

In this work, we focus on the dynamic properties of hydrates during the process of formation and dissociation in sediments of the Shenhu area to examine the hydrate pore habits in the complex porous system. The mineral composition, particle size, and pore size distribution of sediment samples were analyzed to reveal pore structure features. The *in situ* observations of hydrate dynamics were enabled by the low-field nuclear magnetic resonance (LF-NMR) method, which provides a fast and nondestructive way of detecting hydrogen-bearing fluids and has been widely used to measure the water saturation and permeability in hydrate-bearing sediments (Ji et al., 2019; Kuang et al., 2020; Wen et al., 2021). A comparison of permeability results from experiments and theoretical models was performed to examine the dynamic evolution of hydrate saturation and pore morphology in sediments of the Shenhu area. Further insights on favorable conditions for hydrate formation and model applicability are expected to provide.

MATERIALS AND METHODS

Samples

In this work, five representative sediment samples (i.e., W04-1 to W04-5) were acquired from the gas hydrate-bearing sediments in the Shenhu area (**Figure 1**). These samples were depressurized and stored after physical property measurements. For experiments on hydrate formation and dissociation, samples were initially evacuated and then saturated with distilled water at 12 MPa for 48 h.

Pore Structure Analysis of Samples

The characterization of mineral composition, particle size, and pore size was performed in this work. Mineralogical data were analyzed using the X-ray diffraction (XRD) method. The grain size analysis of sediment samples for the nano- or micrograins was performed using the Zetasizer Nano ZS90 particle size analyzer and HELOS-OASIS particle size analyzer, respectively. The ASAP 2460 instrument was used for N_2 adsorption measurements to determine pore size distributions of sediments.

In Situ Measurements of Gas Hydrates

Figure 2 shows a schematic of the LF-NMR monitoring apparatus, which was used to perform the *in situ* hydrate formation and dissociation experiments. The experimental apparatus system mainly comprises an LF-NMR analysis system, a core holder, a gas booster, a confining pressure tracking pump, a refrigeration cycle system, and the gas-liquid separator. The LF-NMR system is a Mini MR60 spectrometer with a magnetic field strength of 0.5 T and resonance frequency of 23 MHz. The confining pressure tracking pump is used to maintain certain confining pressure for CO_2 injection. The refrigeration cycle system contains a circulation pump for cooling the fluorocarbon oil to control the experimental temperature.

In experiments, all the sediment samples were enclosed with heat-shrink tubing as a core with a length of 3.9 cm and a diameter of 2.5 cm. They were saturated with distilled water in the core holder, and then the CO_2 was injected into the core holder with a constant flux until the water was displaced to specific content. The outlet valve of the core holder was then closed, and the CO_2 supplement was enabled by a high-pressure pump to maintain the pore pressure at 4 MPa. During the process, some gases dissolved in water across gas–water interfaces. *In situ* NMR measurements started with decreasing temperature. Temperature controlled by the refrigeration cycle system decreased at a speed of 0.01°C/min from room

temperature to 4°C and then kept stable until the end of hydrate formation. Then, the temperature increased at a speed of 0.02°C/min to 15°C for the hydrate dissociation. Gas permeability of the core was measured before and after the experiment. NMR measurements were performed using the Carr–Purcell–Meiboom–Gill (CPMG) pulse sequence during the experiment. Parameters of the CPMG pulse sequence included the echo number of 18,000, echo spacing of 0.15 ms, and waiting time of 1,000 ms.

Calculation of Hydrate Saturation and Permeability

The cumulative value of NMR signal intensity can quantify the water content and volume fraction in porous media, and the transverse relaxation time (T_2) of water, proportional to the surface-to-volume ratio (S/V), can be used to evaluate the pore structure (Ji et al., 2019). For CO_2 hydrate (CO_2·5.75 H_2O) formation and dissociation, the volume of CO_2 hydrate (V_h) can be calculated by water reduction as follows:

$$V_h = \frac{m_h}{\rho_h} = \frac{\frac{m_{wd}}{18 \times 5.75}(44 + 18 \times 5.75)}{\rho_h}, \quad (1)$$

where m_h is the mass of CO_2 hydrate, m_{wd} is the mass reduction of water, and ρ_h is the density of CO_2 hydrate. CO_2 hydrate saturation is the ratio of hydrate volume and pore volume.

The evolution of permeability subject to hydrate saturation is estimated by experimental data and theoretical models. The SDR method is usually used to calculate permeability from NMR data. It is based on the measured T_2 distribution being a pseudo-pore size distribution during hydrate formation or dissociation. **Eqn. 2** is described as follows:

$$K_{SDR} = C\varnothing^4 T_{2gm}^2, \quad (2)$$

where K is the permeability, Φ is the porosity (%), and T_{2gm} is the logarithmic mean of T_2 distribution (mD). The parameter C in the model is estimated by NMR measurements with known porosity and permeability of samples.

Theoretical permeability models differ from each other by using various assumptions of hydrate pore habits. The parallel capillary model, Kozeny grain model, and Masuda model are used in this paper.

1) Parallel capillary model (Kleinberg, 2003).

This model describing porous media as a bundle of straight, parallel cylindrical capillaries was developed by Kleinberg (2003). In this model, hydrate forms in the center of cylindrical pores, uniformly coating the walls of capillary. With the increase in hydrate saturation, an annular flow path is left for fluid. For the hydrate coating capillary walls model, the permeability can be calculated using **Eqn. 3**:

$$K(S_h) = K_0(1 - S_h)^2, \quad (3)$$

where K_0 is the permeability before hydrate formation and S_h is the hydrate saturation. If hydrate occurs in the center of the capillary model, **Eqn. 4** is used:

$$K(S_h) = K_0\left(1 - S_h^2 + \frac{2(1 - S_h)^2}{\ln(S_h)}\right). \quad (4)$$

2) Kozeny grain model (Spangenberg, 2001).

Spangberg (2001) assumed porous media as Kozeny grain models and hydrate distribution patterns of both coating the grains and occupying pore centers can be calculated. For the former pattern, the permeability is evaluated as shown in **Eqn. 5**:

$$K(S_h) = K_0(1 - S_h)^{n+1}, \quad (5)$$

where the saturation exponent n is 1.5 for $0 < S_h < 0.8$. When $S_h > 0.8$, the saturation exponent diverges. **Eqn. 6** is used to calculate the permeability when hydrate occupies the center of the pore, $n = 0.7S_h + 0.3$:

$$K(S_h) = K_0\frac{(1 - S_h)^{n+2}}{\left(1 + S_h^{0.5}\right)^2}. \quad (6)$$

3) Masuda model.

Masuda model (Masuda et al., 1997) is commonly applied to interpret the relationship between permeability and hydrate saturation as **Eqn. 7**:

$$K(S_h) = K_0(1 - S_h)^N, \quad (7)$$

where N with regard to pore structure is the permeability decreasing index and changes from 2 to 15 (Kumar et al., 2010).

PORE STRUCTURE CHARACTERISTICS OF SEDIMENTS

Mineral Composition Analysis

The XRD analysis of sediment samples shows that the predominant minerals are quartz (30.9%~37.0 wt. %), carbonate minerals (22.8%~30.8 wt. %), and mica (13.6~31.6 wt. %) and are followed by clay minerals. The lower contents of clay minerals were determined in this work compared to previous studies (Li et al., 2019; Wang et al., 2021), which reported the weight percent of clay minerals high to 40% for samples from the SCS.

Grain Size Analysis

The results of the grain size analysis show similar properties of particle size distributions for five sediment samples. The frequency curves of all the samples are unimodal (**Figure 3**) and negatively skewed, with peak values varying over a broad range of 20~40 um (**Figure 3B**). In particular, the median grain size of W04-1, W04-2, W04-3, W04-4, and W04-5 is 5.47, 18.57, 17.09, 11.84, and 17.48 um, respectively. It indicates that the sediments from the SCS mainly comprise clay (< 4 μm) and fine sand grains (4~64 μm). Particle size distributions of nanosized grains also highlight the grains of samples are very fine. The frequency curves are also unimodal with a range of 396~1,106 nm, and peak values of curves vary from 600 to 800 nm (**Figure 3A**).

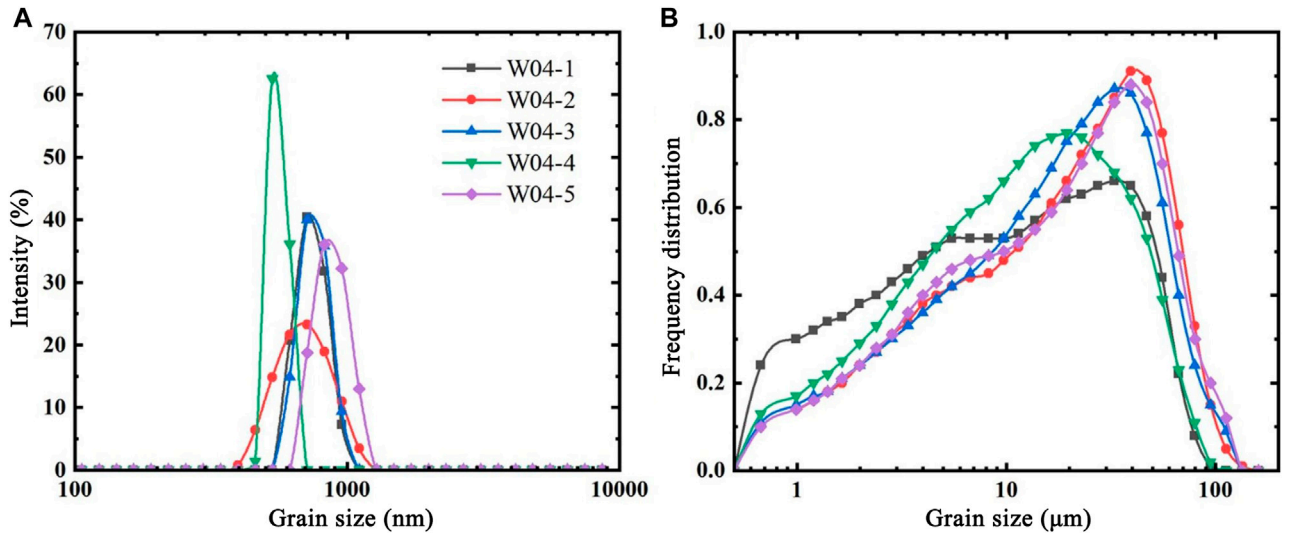

FIGURE 3 | Frequency distribution curves of the particle size of sediment samples.

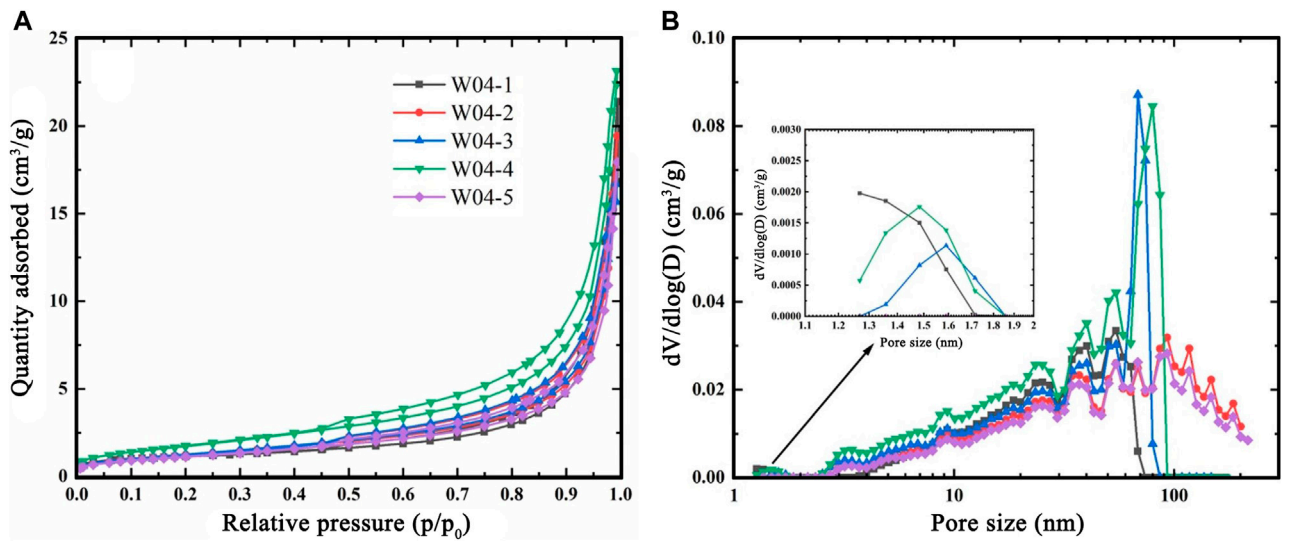

FIGURE 4 | Adsorption and desorption isotherms **(A)** and pore size distributions **(B)** of sediment samples from N_2 adsorption measurements.

Pore Size Analysis

The N_2 adsorption–desorption isotherms of five samples display similar patterns (**Figure 4A**). The adsorption isotherms increase slightly at a relative pressure (p/p_0) <0.45, followed by a sharp increase when p/p_0 is close to 1.0. The hysteresis loops of adsorption–desorption isotherms are indistinctive, which indicates the pore system of sediment samples is composed of cylindrical, wedge-shaped, or slit pores.

Figure 4B shows pore size distributions of W04-1 to W04-5. For W04-1, W04-3, and W04-4, results of pore size with the bimodal distribution mainly range from 1.3 to 80 nm. In particular, the first peak value is 1.27, 1.59, and 1.48 nm, and the second peak value is 54.42, 68.50, and 79.87 nm for W04-1, W04-3, and W04-4, respectively. The pore size curves are unimodal with a peak value of 93.13 nm for W04-2 and W04-5. Based on pore size analysis, a large number of nanopores in these sediments can provide considerable space for hydrate accumulation.

HYDRATE DYNAMICS ANALYSIS AND PERMEABILITY EVOLUTION

Results of NMR Measurements

Figure 5 shows the procedure of the experiments with an increase and then a decrease in the temperature. The whole process can be divided into several periods in terms of the variation of hydrate

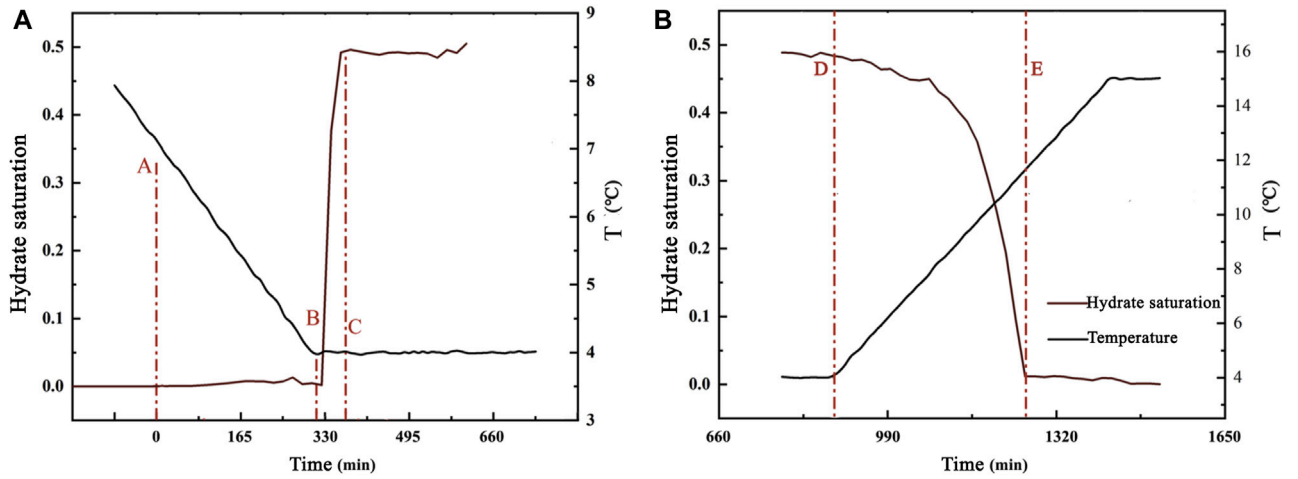

FIGURE 5 | Variations in hydrate saturation during the process of gas hydrate formation **(A)** and dissociation **(B).**

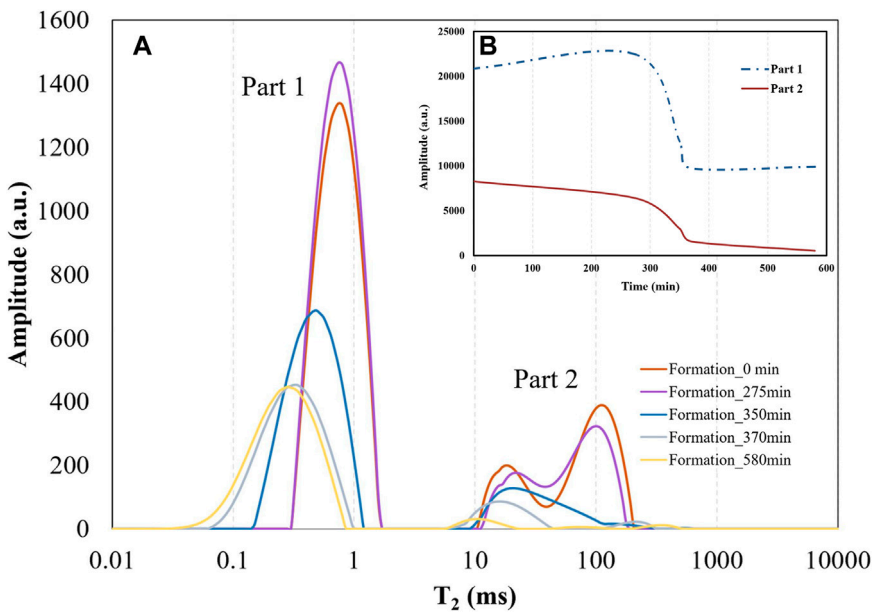

FIGURE 6 | T_2 distribution spectra of NMR **(A)** and cumulative signal of NMR **(B)** during gas hydrate formation.

saturation. For the period A-B, an induction time for hydrate formation is observed with the limited variation of hydrate. During period B-C, the pressure and temperature conditions are favorable for hydrate formation, and hydrate saturation increased rapidly up to 50%. The rate of hydrate formation is around 12%/min, estimated by variations of hydrate saturation (%) over time. The hydrate saturation is almost consistent within the period C-D resulting from the consumption of water and the limited contact between water and gas. After the D point, the temperature increases gradually and results in the dissociation of hydrates. During period D-E, the rate of dissociation gradually increases to 3%/min with the higher temperature. It is because the experimental condition is far away from the phase equilibrium condition, leading to a larger driving force for hydrate dissociation. At the end of the experiments, all the CO_2 hydrates dissociate, and the hydrate saturation decreases to 0.

Evolution of Pore Structure With Hydrate Dynamics

T_2 distribution spectra of NMR provide insights into the pore size distribution of sediments and the change of pore space subjected to the hydrate formation or dissociation. As shown in **Figure 6A**, there are two distinct parts for the initial signal of sediment samples, i.e., Part 1 (0.2~2 ms) and Part 2 (10~300 ms), representing the complex pore structure with mixed grains. At the early stage of

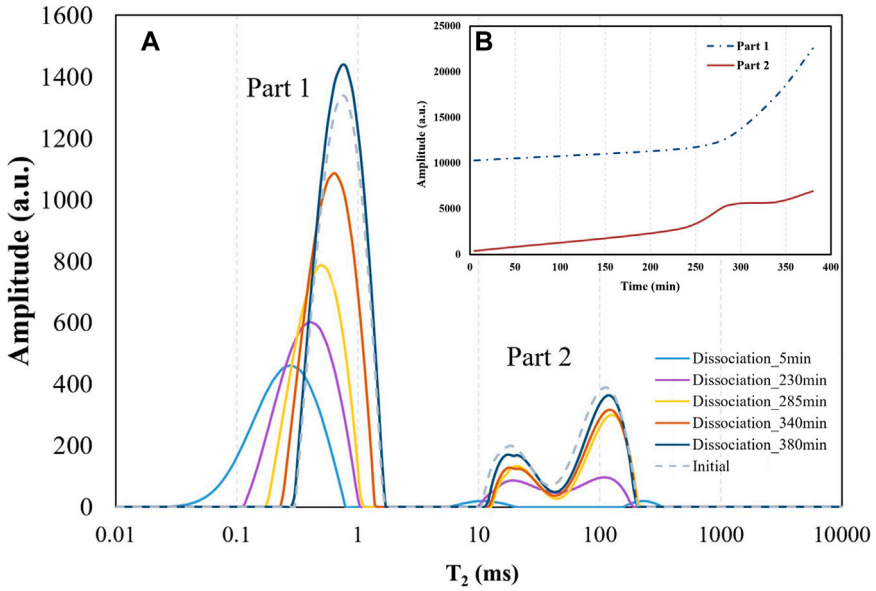

FIGURE 7 | T_2 distribution spectra of NMR **(A)** and cumulative signal of NMR **(B)** during gas hydrate dissociation.

hydrate formation, there is an obvious decrease in Part 2, whereas there is a slight increase in the peak of Part 1. It indicates that the pore space of Part 2 is occupied by the formation of hydrate and leads to a faster relaxation time of the NMR signal. The peak area of Part 2 decreases 40% from 275 to 350 min with a preferential formation of hydrate in larger pores. Some scholars believed that the enhanced performance of heat and mass transfer makes it easier for large pore spaces to achieve nucleation (Qin et al., 2021). With the continuous increase of hydrate saturation, Part 2 became vanished, while Part 1 was still with a low peak at the end of hydrate formation. The phenomenon shows the movement of fluid is quite limited with the presence of hydrates, and thus the local hydrate formation is restrained due to the lack of water or gas.

An opposite tendency of NMR signal variation can be observed in the process of hydrate dissociation (**Figure 7**). The value and width of peaks increase with the hydrate dissociation. Compared to the process of formation, the increase of Part 2 is slightly later than that of Part 1. The rate of hydrate dissociation gradually increases in both Part 1 and Part 2 over time confirmed by the cumulative intensity of the NMR signal. A noticeable difference is shown between the T_2 distribution spectra of the initial situation and the end of dissociation. Similar behaviors have been observed by Lei et al. (2022b). They analyzed microscopic pore characteristics and flowability of five samples from the Shenhu area, showing better connectivity in hydrate-bearing sediment samples after hydrate dissociation compared to samples from the underlying layer. It demonstrates that pore structure may be altered after the hydrate dynamics in both pore size and pore quantity.

Evolution of Permeability With Hydrate Dynamics

Hydrate saturation and permeability in the porous medium were determined by NMR measurements, and the tendency of permeability evolution subjected to the hydrate formation or dissociation is shown in **Figure 8**. With the increase of hydrate saturation, a remarkable decrease in permeability can be observed. It indicates that the permeability of porous media obviously decreases with occupying gas hydrates in pore spaces, and the evolution of permeability differs in terms of the hydrate quantity and distribution. In particular, an order of magnitude lower is in permeability with the hydrate saturation of 32%, while three orders of magnitude are lower with the hydrate saturation of 50% compared to the initial permeability.

By comparing permeability results obtained from experimental data and theory models, different tendencies of permeability evolution are shown in **Figure 8**. Generally, a sharper change of permeability is determined by experimental data at the early stage, while a gentler change at the middle stage is compared to other models. In particular, NMR results show a good agreement with the parallel capillary model (pore-filling) when the hydrate saturation is smaller than 0.1, indicating hydrates prefer to form in the pore central space. Compared to other patterns of hydrate distribution, e.g., a thin film of hydrate coating grain walls, the changes in the permeability are expected to be larger if hydrates occupy flow paths. When the hydrate saturation is larger than 0.3, permeability evolution can be especially captured by the Masuda model (n = 12). Some studies demonstrated that grain-coating hydrates appear to be more common than pore-filling ones with a low porosity and permeability (Lei et al., 2022a). Moreover, a drastic reduction in permeability may occur if formed hydrates plug the pore throats in addition to pore bodies, especially when a high hydrate saturation is in porous media. It is clear that the tendency of permeability evolution is differentiated induced by various patterns of hydrate growth in pores and is more complicated when hybrid patterns exist. In this work, most experimental

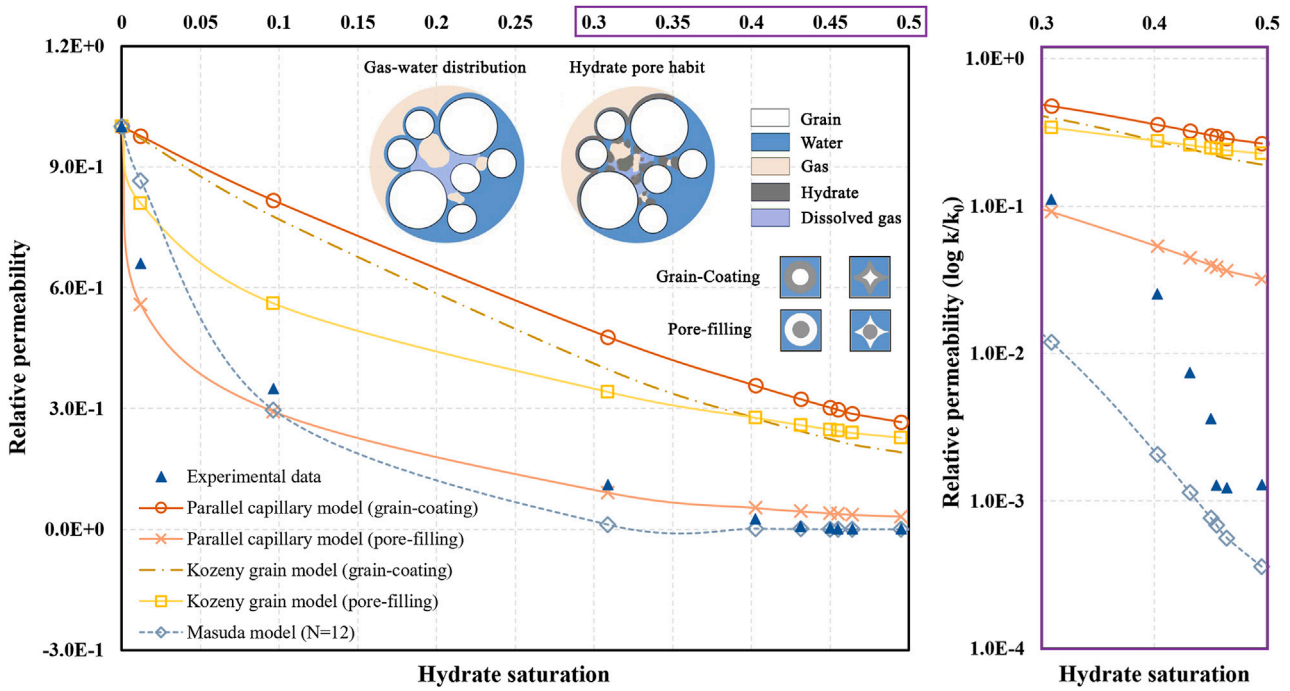

FIGURE 8 | Comparison of permeability evolution from experimental data and theory models.

permeability data points fall between fitted lines from different theoretical permeability models, i.e., the pore wall coating and pore center occupying models. It highlights that hybrid pore habits of hydrates affect the evolution of permeability in hydrate-bearing sediments of the Shenhu area, and a preponderant pattern of hydrate growth changes spatially and temporally.

During the process of hydrate formation and dissociation, pore structure characteristics of sediments influence the hydrate saturation and distribution, as well as gas–water conditions. Previous studies pointed out that various gas–water flow patterns result in excess-gas, excess-water, or dissolved-gas conditions for hydrate formation in sediments and have a profound impact on hydrate growth (Wang et al., 2021). In the excess-gas condition, a limited amount of water mainly cements hydrophilic grain surfaces or contacts, which results in grain-coating hydrates with gas diffusing into water layers. But when the ratio of gas to water is low, the formation of hydrate starts close to trapped gas bubbles or dissolved-gas regions, and gradually exhibits a pore-filling morphology. In this experiment, excess-gas, excess-water, and dissolved-gas conditions coexist in sediments, and gas–water ratios and distributions vary with hydrate dynamics (illustrated in **Figure 8**). Hydrates formed at gas–water interfaces can continuously grow to coat grains or occupy pore central spaces subjected to the specific gas–water condition. In this regard, a theoretical model assuming a single pattern of hydrate growth is expected to fail to predict the hydrate–saturation-dependent permeability in a geosystem in terms of heterogeneous pore structures and gas–water conditions.

CONCLUSIONS

Properties of porous media play a critical role in the formation, dissociation, and occurrence of gas hydrates under natural conditions. In a complex geological media, heterogeneous pore structure will largely complicate the scientific nature of hydrate dynamics during the process of formation and dissociation. This work performed *in situ* observations of pore structure evolution with regard to the changes in hydrate saturation by using LF-NMR measurements. The sediments from the Shenhu area of the SCS with the main components of quartz, calcite, and mica minerals, are composed of clay and fine grains. Nanopores with a range from several to tens of nanometers contribute to the pore space for hydrate growth and accumulation.

In such porous media, gas hydrates gradually form after an induction time; however, they immediately dissociate with an increasing temperature. Estimated by variations of hydrate saturation (%) over time, the rate of hydrate formation is around 12%/min, while the highest rate of dissociation is 3%/min. Because of the occupation of pore space with the hydrate growth, the permeability of sediments decreases obviously with an increase in hydrate saturation. However, the relationship between permeability and saturation is quite complex and cannot be described by theoretical models with a simple assumption of hydrate pore habits. When the saturation is from 20 to 45%, one to three orders of magnitude lower in permeability is determined by experiments, respectively. The tendency of permeability evolution compared to predicted outcomes from permeability models indicates coexistence of both pore-filling and grain-coating hydrate pore morphology

in sediments of the Shenhu area. Moreover, heterogeneous pore structure complicates gas–water conditions in sediments, which leads to spatial and temporal variations in hydrate pore habits. For the improved understanding and predictive capability of hydrate–saturation-dependent permeability, coupled effects of porous media properties and evolution conditions have to be addressed in hydrate-bearing sediments.

DATA AVAILABILITY STATEMENT

The original contributions presented in the study are included in the article/Supplementary Material, further inquiries can be directed to the corresponding author.

AUTHOR CONTRIBUTIONS

QZ, YD, and HZ contributed to the conception and design of the study. LX organized the database. XQ performed the statistical analysis. QZ and HZ wrote the first draft of the manuscript. CL, SL, CM, and HB wrote sections of the manuscript. All authors contributed to manuscript revision, read, and approved the submitted version.

FUNDING

This research was supported by the Key Research Program of the Institute of Geology & Geophysics, CAS (no. IGGCAS-201903), the National Natural Science Foundation of China (No. 51991365), Guangdong Major Project of Basic and Applied Basic Research (No. 2020B0301030003), and China Geological Survey Project (No. DD20211350).

ACKNOWLEDGMENTS

The authors are grateful to the Editor and two reviewers for their critical and constructive reviews.

REFERENCES

Andres-Garcia, E., Dikhtiarenko, A., Fauth, F., Silvestre-Albero, J., Ramos-Fernández, E. V., Gascon, J., et al. (2019). Methane Hydrates: Nucleation in Microporous Materials. *Chem. Eng. J.* 360, 569–576. doi:10.1016/j.cej.2018.11.216

Delli, M. L., and Grozic, J. L. H. (2014). Experimental Determination of Permeability of Porous media in the Presence of Gas Hydrates. *J. Pet. Sci. Eng.* 120, 1–9. doi:10.1016/j.petrol.2014.05.011

Ghaedi, H., Ayoub, M., Bhat, A. H., Mahmood, S. M., Akbari, S., and Murshid, G. (2016). The Effects of Salt, Particle and Pore Size on the Process of Carbon Dioxide Hydrate Formation: A Critical Review. *AIP Conf. Proc.* 1787, 060001. doi:10.1063/1.4968128

Heeschen, K. U., Schicks, J. M., and Oeltzschner, G. (2016). The Promoting Effect of Natural Sand on Methane Hydrate Formation: Grain Sizes and mineral Composition. *Fuel* 181, 139–147. doi:10.1016/j.fuel.2016.04.017

Ji, Y., Hou, J., Cui, G., Lu, N., Zhao, E., Liu, Y., et al. (2019). Experimental Study on Methane Hydrate Formation in a Partially Saturated sandstone Using Low-Field NMR Technique. *Fuel* 251, 82–90. doi:10.1016/j.fuel.2019.04.021

Kang, D. H., Yun, T. S., Kim, K. Y., and Jang, J. (2016). Effect of Hydrate Nucleation Mechanisms and Capillarity on Permeability Reduction in Granular Media. *Geophysical Research Letters* 43 (17), 9018–9025.

Kleinberg, R. L. (2003). Deep Sea NMR: Methane Hydrates Growth Habit in Porous media and its Relationship to Hydraulic Permeability, deposit Accumulation, and Submarine Slope Stability[J]. *J. Geophys. Res. Solid Earth* 108 (B10), 2508. doi:10.1029/2003jb002389

Kossel, E., Deusner, C., Bigalke, N., and Haeckel, M. (2018). The Dependence of Water Permeability in Quartz Sand on Gas Hydrate Saturation in the Pore Space. *J. Geophys. Res. Solid Earth* 123 (2), 1235–1251. doi:10.1002/2017jb014630

Kuang, Y., Zhang, L., Song, Y., Yang, L., and Zhao, J. (2020). Quantitative Determination of Pore-structure Change and Permeability Estimation under Hydrate Phase Transition by NMR. *AIChE J.* 66 (4), e16859. doi:10.1002/aic.16859

Kumar, A., Maini, B., Bishnoi, P. R., Clarke, M., Zatsepina, O., and Srinivasan, S. (2010). Experimental Determination of Permeability in the Presence of Hydrates and its Effect on the Dissociation Characteristics of Gas Hydrates in Porous Media[J]. *J. Pet. Sci. Eng.* 70 (1/2), 114–122. doi:10.1016/j.petrol.2009.10.005

Kumar Saw, V., Udayabhanu, G., Mandal, A., and Laik, S. (2015). Methane Hydrate Formation and Dissociation in the Presence of Silica Sand and Bentonite Clay. *Oil Gas Sci. Technol. - Rev. IFP Energies Nouvelles* 70, 1087–1099. doi:10.2516/ogst/2013200

Lei, X., Yao, Y., Luo, W., and Wen, Z. (2022a). Permeability Change in Hydrate Bearing Sediments as a Function of Hydrate Saturation: A Theoretical and Experimental Study. *J. Pet. Sci. Eng.* 208, 109449. doi:10.1016/j.petrol.2021.109449

Lei, X., Yao, Y., Qin, X., Lu, C., Luo, W., Wen, Z., et al. (2022b). Pore Structure Changes Induced by Hydrate Dissociation: An Example of the Unconsolidated Clayey-Silty Hydrate Bearing Sediment Reservoir in the South China Sea. *Mar. Geology.* 443, 106689. doi:10.1016/j.margeo.2021.106689

Letcher, M. T. (Editor) (2020). *Future Energy: Improved, Sustainable and Clean Options for Our planet[M]* (Amsterdam, Netherlands: Elsevier), 111–131.

Liang, H., Song, Y., Chen, Y., and Liu, Y. (2011). The Measurement of Permeability of Porous Media With Methane Hydrate. *Petroleum Science and Technology, 2011* 29, 79–87. doi:10.1016/j.margeo.2021.106689

Liang, J. Q., Wei, J. G., Bigalke, N., Roberts, J., Schultheiss, P., Holland, M., et al. (2017). "Laboratory Quantification of Geomechanical Properties of Hydrate-Bearing Sediments in the Shenhu Area of the South China Sea at *In-Situ* Conditions," in Proceedings of the 9th International Conference on Gas Hydrates, Denver, 30.

Li, J., Lu, J. a., Kang, D., Ning, F., Lu, H., Kuang, Z., et al. (2019). Lithological Characteristics and Hydrocarbon Gas Sources of Gas Hydrate-Bearing Sediments in the Shenhu Area, South China Sea: Implications from the W01B and W02B Sites. *Mar. Geology.* 408, 36–47. doi:10.1016/j.margeo.2018.10.013

Li, Z.-d., Tian, X., Li, Z., Xu, J.-z., Zhang, H.-x., and Wang, D.-j. (2020). Experimental Study on Growth Characteristics of Pore-Scale Methane Hydrate. *Energ. Rep.* 6, 933–943. doi:10.1016/j.egyr.2020.04.017

Liu, W., Wang, S., Yang, M., Song, Y., Wang, S., and Zhao, J. (2015). Investigation of the Induction Time for THF Hydrate Formation in Porous media. *J. Nat. Gas Sci. Eng.* 24, 357–364. doi:10.1016/j.jngse.2015.03.030

Lu, C., Qin, X., Mao, W., Ma, C., Geng, L., Yu, L., et al. (2021b). Experimental Study on the Propagation Characteristics of Hydraulic Fracture in Clayey-Silt Sediments. *Geofluids* 2021, 6698649. doi:10.1155/2021/6698649

Lu, C., Qin, X., Yu, L., Geng, L., Mao, W., Bian, H., et al. (2021a). The Characteristics of Gas-Water Two-phase Radial Flow in Clay-Silt Sediment and Effects on Hydrate Production. *Geofluids* 2021 (3), 1–14. doi:10.1155/2021/6623802

Masuda, Y. S., Naganawa, S., Ando, S., and Sato, K. (1997). "Numerical Calculation of Gas Production Performance From Reservoirs Containing Natural Gas Hydrates; Paper SPE 38291," in Proceedings, Western Regional Meeting, June, 25–27.

Prasad, P. S. R. (2015). Methane Hydrate Formation and Dissociation in the Presence of Hollow Silica. *J. Chem. Eng. Data* 60, 304–310. doi:10.1021/je500597r

Qin, Y., Pan, Z., Liu, Z., Shang, L., and Shang, L. (2021). Influence of the Particle Size of Porous Media on the Formation of Natural Gas Hydrate: A Review[J]. *Energy & Fuels* 35 (15), 11640. doi:10.1021/acs.energyfuels.1c00936

Ren, X., Guo, Z., Ning, F., and Ma, S. (2020). Permeability of Hydrate-Bearing Sediments. *Earth-Science Rev.* 202, 103100. doi:10.1016/j.earscirev.2020.103100

Shen, P., Li, G., Li, B., and Li, X. (2020). Coupling Effect of Porosity and Hydrate Saturation on the Permeability of Methane Hydrate-Bearing Sediments. *Fuel* 269, 117425. doi:10.1016/j.fuel.2020.117425

Siangsai, A., Rangsunvigit, P., Kitiyanan, B., Kulprathipanja, S., and Linga, P. (2015). Investigation on the Roles of Activated Carbon Particle Sizes on Methane Hydrate Formation and Dissociation . *Chemical Engineering Science* 126, 383–389.

Sloan, E. D. (2003). Fundamental Principles and Applications of Natural Gas Hydrates. *Nature* 426 (6964), 353–359. doi:10.1038/nature02135

Song, G., Li, Y., and Sum, A. K. (2020). Characterization of the Coupling between Gas Hydrate Formation and Multiphase Flow Conditions. *J. Nat. Gas Sci. Eng.* 83, 103567. doi:10.1016/j.jngse.2020.103567

Spangenberg, E. (2001). Modeling of the Influence of Gas Hydrate Content on the Electrical Properties of Porous Sediments. *J. Geophys. Res.* 106 (B4), 6535–6548. doi:10.1029/2000jb900434

Su, M., Yang, R., Wang, H., Sha, Z., Liang, J., Wu, N., et al. (2016). Gas Hydrates Distribution in the Shenhu Area, Northern South China Sea: Comparisons Between the Eight Drilling Sites With Gas-Hydrate Petroleum System. *Geol. Acta.* 14 (2), 79–100.

Sun, J., Dong, H., Arif, M., Yu, L., Zhang, Y., Golsanami, N., et al. (2021). Influence of Pore Structural Properties on Gas Hydrate Saturation and Permeability: a Coupled Pore-Scale Modelling and X-ray Computed Tomography Method. *J. Nat. Gas Sci. Eng.* 88, 103805. doi:10.1016/j.jngse.2021.103805

Wang, P. (2019). *Hydrate Formation Characteristic under Gas Migration in Porous medium[D]*. Dalian, China: Dalian University of Technology.

Wang, Q., Chen, X., Zhang, L., Wang, Z., Wang, D., and Dai, S. (2021). An Analytical Model for the Permeability in Hydrate-bearing Sediments Considering the Dynamic Evolution of Hydrate Saturation and Pore Morphology. *Geophys. Res. Lett.* 48 (8), e2021GL093397. doi:10.1029/2021gl093397

Wen, Z., Yao, Y., Luo, W., and Lei, X. (2021). Memory Effect of CO2-hydrate Formation in Porous media. *Fuel* 299, 120922. doi:10.1016/j.fuel.2021.120922

Yin, Z., Moridis, G., Chong, Z. R., Tan, H. K., and Linga, P. (2018). Numerical Analysis of Experimental Studies of Methane Hydrate Dissociation Induced by Depressurization in a sandy Porous Medium. *Appl. Energ.* 230, 444–459. doi:10.1016/j.apenergy.2018.08.115

Zhang, L., Sun, M., Sun, L., Yu, T., Song, Y., Zhao, J., et al. (2019). *In-situ* Observation for Natural Gas Hydrate in Porous Medium: Water Performance and Formation Characteristic. *Magn. Reson. Imaging* 65, 166–174. doi:10.1016/j.mri.2019.09.002

Conflict of Interest: The authors declare that the research was conducted in the absence of any commercial or financial relationships that could be construed as a potential conflict of interest.

Publisher's Note: All claims expressed in this article are solely those of the authors and do not necessarily represent those of their affiliated organizations or those of the publisher, the editors, and the reviewers. Any product that may be evaluated in this article, or claim that may be made by its manufacturer, is not guaranteed or endorsed by the publisher.